

Numerical Study on Flame Geometric Characteristics of Ammonia-Fueled Small Boiler

Kunfeng Sun^{1,*}

¹School of Smart Energy & Environment, Zhongyuan University of Technology, Zhengzhou, China

*Corresponding author: Kunfeng Sun (Email: skf0558@sina.com)

Abstract: Amidst global efforts to cut carbon emissions, the carbon-neutral fuel sector is at a crossroads of opportunity and challenge. The pursuit of clean, sustainable energy alternatives is critical. Ammonia, with its zero-carbon and hydrogen-rich profile, is emerging as a promising clean fuel, yet its combustion behavior in industrial boilers demands further study. This paper presents a numerical analysis of the flame geometry characteristics of ammonia combustion at an equivalence ratio of 1. The study delineates the dimensions of the flame, specifically its diameter and length, offering valuable insights that can inform the design of industrial boilers. This research contributes to the broader understanding of ammonia's role in the transition towards more sustainable energy solutions in industrial settings.

Keywords: Ammonia, Numerical simulation, Boiler, Geometric characteristics.

1. Introduction

The extensive utilization of fossil fuels has resulted in a significant escalation of carbon dioxide emissions, thereby intensifying the greenhouse effect. Consequently, there is an urgent need to ameliorate the detrimental environmental consequences of carbon emissions. To this end, the scientific community is vigorously pursuing sustainable and renewable energy alternatives [1, 2]. Among these, hydrogen energy has garnered considerable interest due to its inherent cleanliness, yet the challenge of its safe and practical storage must be surmounted to realize a global hydrogen economy [3].

Ammonia, as an emerging energy vector, has increasingly piqued interest owing to its distinctive advantages. It is characterized as a "zero-carbon hydrogen-rich" clean energy source with the potential to supplant fossil fuels [4]. Despite its toxicity, ammonia is less prone to ignition compared to hydrogen and gasoline. The merits of ammonia include its established industrial production processes, its amenability to storage and transportation, and the fact that its combustion yields only nitrogen and water, thereby achieving zero carbon emissions. Furthermore, ammonia boasts a high hydrogen content, making it an efficient hydrogen carrier. Its low liquefaction pressure at room temperature facilitates storage and transportation, and its volumetric energy density surpasses that of hydrogen, rivaling that of gasoline and diesel. It also exhibits a high octane rating and superior anti-knock properties [5].

Nevertheless, the use of ammonia as a fuel is not without its challenges. These include potential instability during combustion and the risk of high NO_x emissions upon burning [6]. Additionally, the combustion characteristics of ammonia in various combustion apparatuses are a subject of ongoing research. The objective of this study is to investigate the flame geometry of ammonia combustion in small-scale boilers through numerical simulation. This research aims to provide a scientific foundation and technical guidance for the integration of ammonia into power generation equipment.

2. Problem Description

2.1. Computation Domain and Mesh

This article utilizes a burner shown in Figure 1. Considering the symmetry of the burner chamber, the computational domain is simplified into a two-dimensional axial symmetry model. The overall dimensions of the burner are a length of 4000mm and an inner diameter of 500mm. The two-dimensional mesh is made up of 46700 elements, this mesh criterion was taken from Ref[19]. The computational model is illustrated in Figure 1.

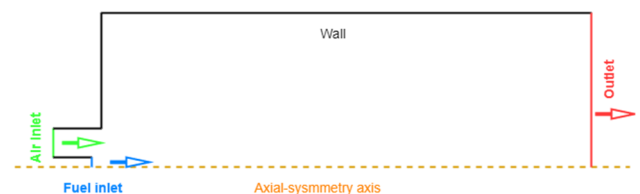


Figure 1. Schematic of the burner chamber

2.2. Theoretical Background

Numerical calculations of combustion require fundamental control equations, including the continuity equation, momentum conservation equation, energy conservation equation, and chemical species transport equation [7,8, 9]. In this study, for the combustion in a gas boiler, the Navier-Stokes (N-S) equations are employed to describe fluid flow, the RNG *k*-epsilon (*k*-*e*) equations are utilized as the turbulence model, and the non-premix model is adopted as the combustion model. Radiation calculation adopts DO model [8]. The SIMPLE algorithm is used as the pressure-velocity coupling method. The discretization of each equation adopts a second-order precision format.

The continuity equation is written in the following form:

$$\frac{\partial \rho}{\partial t} + \frac{\partial(\rho u_i)}{\partial x_i} = 0 \quad (1)$$

Where, ρ is density, u_i are velocity components.

The momentum equations are written:

$$\frac{\partial(\rho u_i)}{\partial t} + \frac{\partial(\rho u_i u_j)}{\partial x_j} = \frac{\partial}{\partial x_i} \left[\mu \frac{\partial u_i}{\partial x_i} - \rho \overline{u'_i u'_j} \right] - \frac{\partial p}{\partial x_i} + S_i \quad (2)$$

Where, μ is Dynamic viscosity, $\overline{u'_i}$ are fluctuating velocity components, p is pressure, S_i are source terms.

The energy equation for the Non_Premix combustion Model is written[7]:

$$\frac{\partial}{\partial t}(\rho H) + \nabla \cdot (\rho \vec{v} H) = \nabla \cdot \left(\frac{k_{eff}}{C_p} \nabla H \right) + S_h \quad (3)$$

Where, $H = \sum_j Y_j H_j$ is total enthalpy, k_{eff} is the effective conductivity ($k + k_t$), where k_t is the turbulent thermal conductivity.

Turbulence models:

This study focuses on the combustion of gas boilers, where the gas flow inside the furnace is turbulent flow. RNG k- ϵ turbulence model commonly used in combustion calculations, these models consist of two equations: turbulent kinetic energy equation and dissipation rate equation. The equations expression is as follows:

$$\frac{\partial(\rho k)}{\partial t} + \frac{\partial(\rho k u_i)}{\partial x_i} = \frac{\partial}{\partial x_j} \left[\left(\mu + \frac{\mu_t}{\sigma_k} \right) \frac{\partial k}{\partial x_j} \right] + G_k + G_b - \rho \epsilon - Y_M + S_k \quad (4)$$

$$\frac{\partial(\rho \epsilon)}{\partial t} + \frac{\partial(\rho \epsilon u_i)}{\partial x_i} = \frac{\partial}{\partial x_j} \left[\left(\mu + \frac{\mu_t}{\sigma_\epsilon} \right) \frac{\partial \epsilon}{\partial x_j} \right] + C_{1\epsilon} \frac{\epsilon}{k} (G_k + C_{3\epsilon} G_b) - C_{2\epsilon} \rho \frac{\epsilon^2}{k} + S_\epsilon \quad (5)$$

In above equations, G_k represents the generation of turbulence kinetic energy due to the mean velocity gradients, G_b is the generation of turbulence kinetic energy due to buoyancy,

Y_m represents the contribution of the fluctuating dilatation in compressible turbulence to the overall dissipation rate and S_k, S_ϵ are user-defined source terms. $C_{1\epsilon}, C_{2\epsilon}, C_{3\epsilon}$ and $\sigma_k, \sigma_\epsilon$ are constants.

The species transport equations are written:

$$\frac{\partial(\rho Y_i)}{\partial t} + \frac{\partial(\rho u_j Y_i - J_i)}{\partial x_j} = R_i + S_i \quad (6)$$

Where, where R_i is the net rate of production of species by chemical reaction and S_i is the rate of creation by addition from the dispersed phase plus any user-defined sources. J_i is the diffusion flux of species i .

The Favre mean (density-averaged) mixture fraction equation is

$$\frac{\partial}{\partial t}(\rho \bar{f}) + \nabla \cdot (\rho \vec{v} \bar{f}) = \nabla \cdot \left(\left(\frac{k}{C_p} + \frac{\mu_t}{\sigma_f} \right) \nabla \bar{f} \right) + S_m + S_{user} \quad (7)$$

where k is laminar thermal conductivity of the mixture, C_p is the mixture specific heat, σ_f is the Prandtl number, and μ_t is the turbulent viscosity.

The source term S_m is due solely to transfer of mass into the gas phase from liquid fuel droplets or reacting particles. S_{user} is any user-defined source term.

The conservation equation for the mixture fraction variance is :

$$\frac{\partial}{\partial t}(\rho \overline{f'^2}) + \nabla \cdot (\rho \vec{v} \overline{f'^2}) = \nabla \cdot \left(\left(\frac{k}{C_p} + \frac{\mu_t}{\sigma_f} \right) \nabla \overline{f'^2} \right) + C_g \mu_t \cdot (\nabla \bar{f})^2 - C_d \rho \frac{\epsilon}{k} \overline{f'^2} + S_{user} \quad (8)$$

where $f' = f - \bar{f}$ is the mixture fraction variance. The default values for the constants σ_f, C_g , and C_d are 0.85, 2.86, and 2.0, respectively, and S_{user} is any user-defined source term.

2.3. Boundary and Initial Conditions

Flow rate and mass flow inlet conditions are selected for air inlet, swirling speed also be considered for air flow, Turbulent intensity is set to 10%. Under different working conditions, the molar ratio of hydrogen in the fuel is shown in Table 1.

Fuel inlet are set to velocity inlet conditions, Turbulent intensity is set to 10%, The exit boundary condition is set as pressure outlet, Turbulent intensity is set to 2%[20].

The circumferential wall is set as a constant temperature boundary, and other walls are set as adiabatic boundary.

Table 1. Velocity of fuel flow

Index	Velocity(m/s)	Index	Velocity(m/s)
1	35	4	20
2	30	5	15
3	25		

3. Chemical-kinetic Modeling

At present, many mechanisms of ammonia combustion have been studied by scholars at home and abroad, including the miller model [19], the Konnov [9] model, and the Hadi Nozari [10, 11] mechanism model. To study the combustion of ammonia at high temperatures and pressures, Song et al. [12] proposed an improved mechanism. Following Song's mechanism, Otomo et al. [13] developed a newer kinetic reaction mechanism, including flame and flame-related reactions. Duynslaegher et al. [14] studied GRI [15], San Diego [16], Lindstedt [17], etc., and found that Konnov's mechanism was consistent under low pressure conditions.

In order to improve the modeling accuracy, Duynslaegher et al. studied a series of mechanisms and obtained a simplified mechanism that was in good agreement with the previous measurements.

In this paper, computational simulations were conducted utilizing the PFR model (shown in Table 2) within the Chemkin Pro software suite [18].

Table 2. Reaction steps and corresponding rate constant data used in the model Mechanism for NH₃/air combustion, Parameters for use in the Arrhenius expression $k = AT^b \exp(-E/(RT))$, And the coefficients A ,b,E with units in cm, mol, s, cal.

Index	Reactions	A	b	E
1	NH ₃ +M=NH ₂ +H+M	0.920E+16	0	84800
2	NH ₃ +H=NH ₂ +H ₂	0.246E+14	0	17071
3	NH ₃ +O=NH ₂ +OH	0.150E+13	0	6040
4	NH ₂ +OH=NH+H ₂ O	0.125E+14	0	2200
5	NH ₃ +OH=NH ₂ +H ₂	0.325E+13	0	2120
6	H+HNO=NH+OH	0.200E+12	0.5	1300
7	HNO+M=H+NO+M	0.300E+17	0	48680
8	HNO+OH=NO+H ₂ O	0.360E+14	0	0
9	NH ₂ +HNO=NH ₃ +N	0.500E+14	0	1000
10	NH ₂ +NO=NNH+OH	0.468E+20	-2.46	1876
11	NH ₂ +NO=N ₂ +H ₂ O	0.702E+20	-2.46	1876
12	NH+O ₂ =HNO+O	0.112E+13	0	3250
13	NNH+M=N ₂ +H+M	0.200E+15	0	20000
14	NNH+NO=N ₂ +HNO	0.500E+14	0	0
15	NNH+OH=N ₂ +H ₂ O	0.300E+14	0	0
16	NH ₂ +NH ₂ =NH ₃ +N	0.630E+13	0	10000
17	CO+OH=CO ₂ +H	0.151E+08	1.3	-758
18	H ₂ +OH=H ₂ O+H	0.520E+14	0	6500
19	H+O ₂ =OH+O	0.719E+17	-0.861	16523
20	O+H ₂ =OH+H	0.180E+11	1	8826
21	2OH=O+H ₂ O	0.170E+07	2.03	-1190
22	H ₂ +M=H+H+M	0.223E+13	0.5	92600
23	H+OH+M=H ₂ O+M	0.750E+24	-2.6	0

5. Results and Discussion

In this work, a non-premixed combustion model was employed to initially derive the PDF average mixing function lookup table, as depicted in Figure 2, which illustrates a two-dimensional schematic diagram. Subsequent numerical computations were conducted for five distinct operational conditions, each with an equivalence ratio of 1, yielding a temperature distribution map of the boiler's thermal field. The

numerical methodology was utilized to simulate the flame structure of ammonia's non-premixed combustion, with Figures 3 to 7 presenting the temperature contours. This approach aligns with the detailed chemical kinetic modeling of ammonia oxidation, as discussed by Otomo et al. , and contributes to the understanding of flame dynamics in non-premixed ammonia combustion systems.

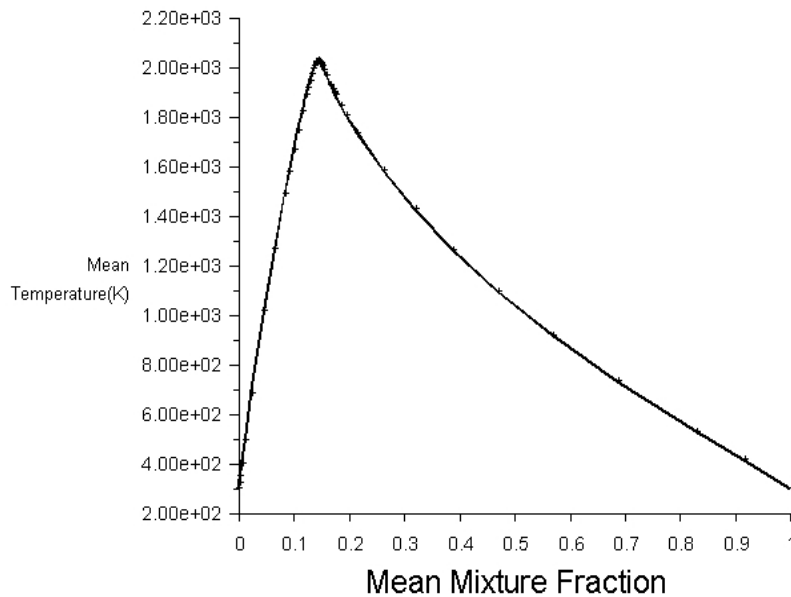


Figure 2. PDF average mixing function lookup table

From the PDF lookup table, it can be seen that the maximum temperature for ammonia combustion is

approximately 2000K. From the temperature contour, it can be seen that the shape of the flame is similar, but the size is

different. As the power increases, the length and diameter of the flame also increase. The contour maps of temperature at

different powers are shown in Figures 2 to 6.

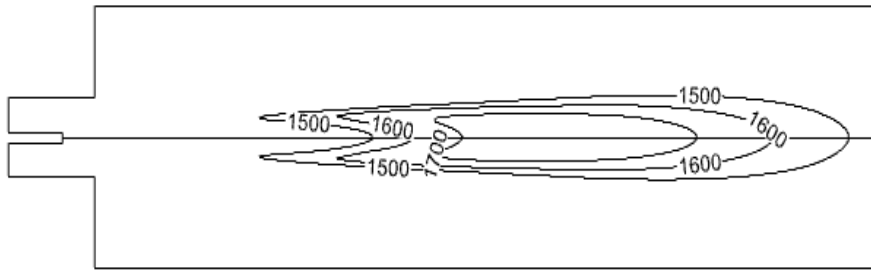


Figure 3. Temperature contour (56kW)

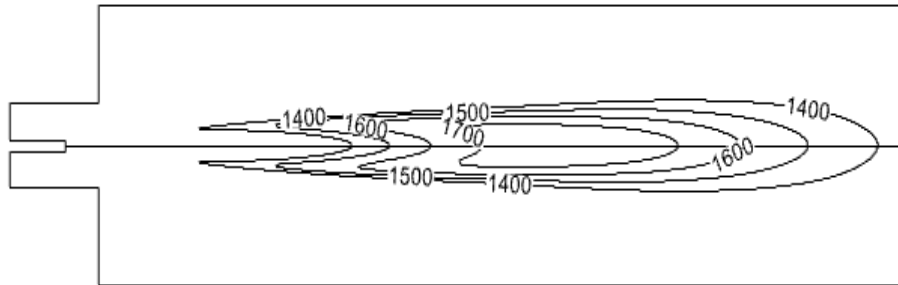


Figure 4. Temperature contour (48kW)

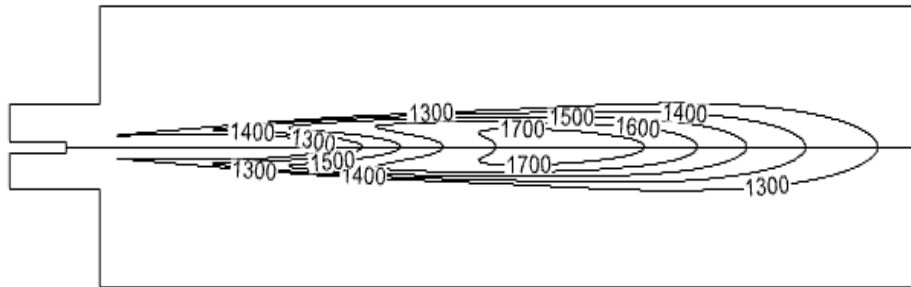


Figure 5. Temperature contour (40kW)

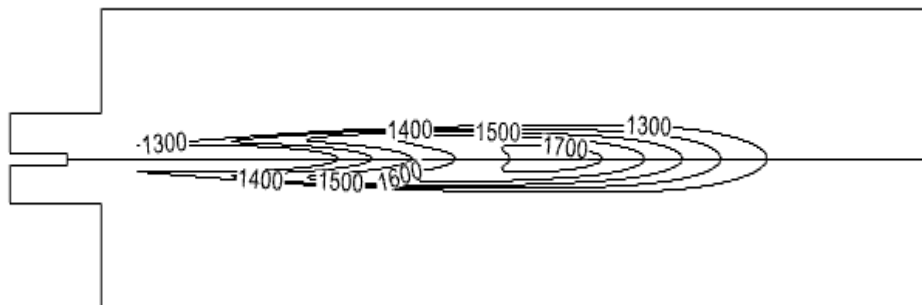


Figure 6. Temperature contour (32kW)

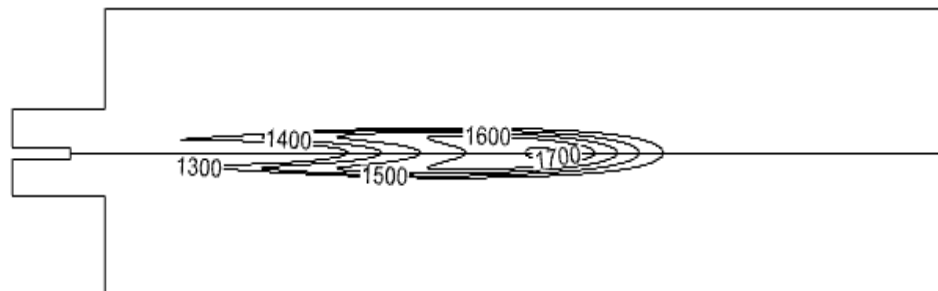


Figure 7. Temperature contour (24kW)

By controlling the boundary conditions, specifically the fuel inlet velocity, a range of power outputs is simulated

within the combustion chamber. The total sensible heat transfer rate within the system is meticulously calculated

using the flux report, which facilitates the determination of the corresponding power value for each scenario. Utilizing the acquired data and cloud map analysis, the flame length

and flame diameter under these specific operating conditions are subsequently calculated.

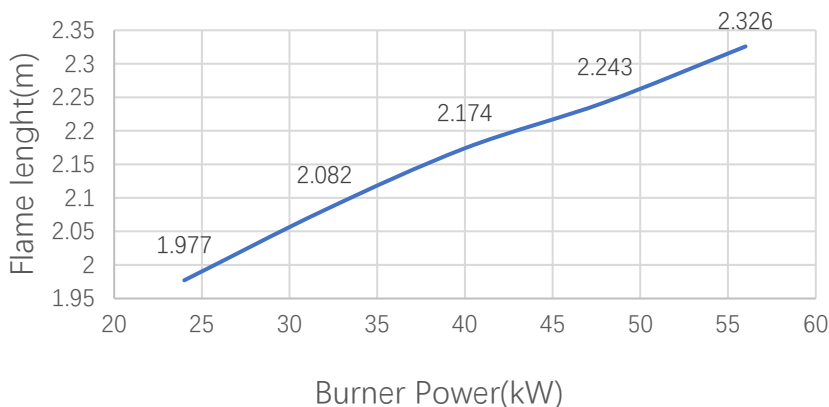


Figure 8. Flame length and burner power correlation curve

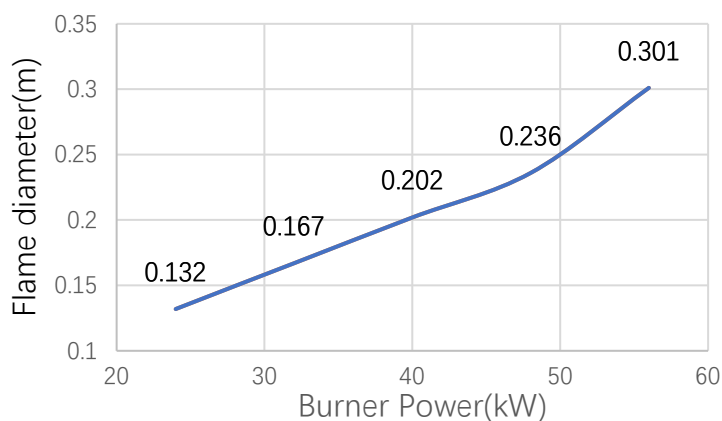


Figure 9. The relationship between flame diameter and burner power

This comprehensive approach enables the generation of a relationship curve between flame length, flame diameter, and power output, as illustrated in Figures 8 and Figures 9. Such an analysis is crucial for optimizing combustion efficiency and can inform strategies for power control in practical applications.

6. Conclusion

As a carbon-free fuel and an excellent hydrogen carrier, the combustion characteristics of NH_3 in industrial boiler combustion need to be studied in detail. In this paper, the turbulent combustion of ammonia in a small boiler is numerically calculated by using the PDF model of non-premixed combustion, and the Chemkin suite PFR ammonia combustion mechanism is applied. The combustion environment of the industrial boiler was simulated under atmospheric pressure conditions, and the grid model was established and the grid independence check was carried out to determine the appropriate grid model, and the temperature fields of ammonia combustion flames of different powers under five working conditions were obtained for the combustion of ammonia in the air, and the geometric characteristics of the flames under different powers could be intuitively seen through comparison.

1) The temperature of ammonia combustion is generally low, and the maximum flame temperature is about 2000K. Therefore, from an industrial point of view, ammonia-doped

combustion may be more promising, and this will be optimized in the next step.

2) As the amount and power of fuel increases, the flame size increases.

3) The diameter and length of the flame vary approximately linearly at the same equivalent ratio.

In the future, it is necessary to compare the flame size of ammonia combustion under different equivalent ratios, and it is necessary to use different ammonia combustion mechanisms to compare, so as to obtain more reasonable and accurate results to meet the requirements of industrial design.

References

- [1] LAI Shini, J.L.L.J., Research progress of ammonia blended fossil fuel. *Chemical Industry and Engineering Progress*. 42(9): p. 4603-4615.
- [2] Research progress on combustion characteristics of new zero carbon ammonia fuel. *Journal of Huazhong University of Science and Technology(Natural Science Edition)*, 2022. 50(7): p. 18.
- [3] Al, Z.S.Y.W., Research progress of ammonia combustion. *Proceedings of the CSEE*, 2021. 41(12): p. 4164-4181.
- [4] TAN Houzhang, Z.S.Y.W., Economic Analysis of Ammonia and Research Progress of Coal-ammonia Co-firing. *Proceedings of CSEE*, 2023. 43(1): p. 181-190.

- [5] Gao Zhengping, T.A.L.T., Recent advances on ammonia combustion technology for zero-carbon power. *Clean Coal Technology*, 2022. 28(3): p. 173-184.
- [6] LIU Feng, F.S.Z.B., Advances in process characteristics and mechanisms of ammonia combustion and co-firing. *Chemical Industry and Engineering*, 2023. 40(6): p. 107-118.
- [7] Ansys Fluent Theory Guide. 2017: Ansys Inc .
- [8] Chunjie, S.Z.L.L., Algebraic second-order moment model for simulation of turbulent non-premixed combustion. *CIESC Journal*, 2014. 65(2): p. 415-421.
- [9] Konnov, A.A., Implementation of the NCN pathway of prompt-NO formation in the detailed reaction mechanism. *Combust. Flame*, 2009. 156: p. 2093–2105.
- [10] Hadi Nozari, A.K., Numerical study of combustion characteristics of ammonia as a renewable fuel and establishment of reduced reaction mechanisms. *Fuel*, 2015. 159: p. 223-233.
- [11] Meyer, T., et al., Ammonia Combustion with Near-zero Pollutant Emissions, in *In NH3 Congress*. 2011: Iowa, USA.
- [12] Song, Y., et al., Ammonia oxidation at high pressure and intermediate temperatures. *Fuel*, 2016. 181: p. 358–365.
- [13] Junichiro Otomo, M.K.T.M., Chemical kinetic modeling of ammonia oxidation with improved reaction mechanism for ammonia/air and ammonia/hydrogen/air Chemical kinetic modeling of ammonia oxidation with improved reaction mechanism for ammonia/air and ammonia/hydrogen/air. *International Journal of Hydrogen Energy*, 2018. 43(5): p. 3004-3014.
- [14] Duynslaegher, C., et al., Modeling of ammonia combustion at low pressure. *Combust. Flame*, 2012. 159: p. 2799–2805.
- [15] Gregory, P.S., et al., GRI-Mech 3.0. 2020.
- [16] Mechanical And Aerospace Engineering Combustion Research, U.O.C.A., *Chemical-Kinetic Mechanisms for Combustion Applications*. 2020.
- [17] Lindstedt, R.P., F.C. Lockwood and M.A. Selim, Detailed Kinetic Modelling of Chemistry and Temperature Effects on Ammonia Oxidation. *Combust. Sci. Technol.*, 1994. 99: p. 253-276.
- [18] Ansys Chemkin. 2017: Ansys Inc.
- [19] F.Dinkelacker, B.Manickam, S.P.R: Modelling and simulation of lean premixed turbulent methane/hydrogen/air flames with an effective Lewis number approach. *Combust and Flame*, Vol 158 (2011) No.9 ,p.1742-1749.
- [20] James A. Miller, Craig T. Bowman. Mechanism and modeling of nitrogen chemistry in combustion [J].*Progress in Energy and Combustion Science*, 1989, 15:287-338.